Spatial Distribution of the Reflected Laser Light at the Experimental Chamber Wall

Yekaterina Merkulova

Spatial Distribution of the Reflected Laser Light at the Experimental Chamber Wall

Yekaterina Merkulova
Advisor: Dr. Jacques Delettrez

Laboratory For Laser Energetics
University of Rochester

Summer High School Research Program

A computer program was created to calculate the distribution of the reflected laser light along the target chamber wall. This is needed to assess the accuracy with which the total reflected light can be estimated from the energy measurement in single detectors covering a small area of the wall. The program generates a grid for the target chamber wall and the angular distribution of the reflected light relative to the axis of a beam. This distribution is transposed from the frame of the rays to the frame of the chamber wall. A search is then performed to map the intensity distribution from the 60 OMEGA beams on the target chamber wall grid. Preliminary results show that there exists a level of non-uniformity of about ±5%.

Introduction

The energy absorbed by targets irradiated by the 60 OMEGA beams is obtained by measuring the reflected energy with calorimeters. However the techniques used in these experiments sample small areas on the chamber wall and assume that the light is reflected uniformly on the chamber wall. Since discrepancies have been discovered between these experiments and simulations, it is necessary to test that assumption. A computer program was written to calculate and map the intensity distribution of the reflected laser light. Input data came from simulations that were carried out with the one-dimensional, hydrodynamic code, LILAC.

Background

The computer program was written based on ray tracing. This method is simpler than direct modeling of the interaction of the laser with the target, and is used to determine the absorption of the laser light by the target. Ray tracing is done by dividing each beam into concentric, circular rays. For this simulation, 200 rays per beam were used. Each ray is followed from the beam, into the target (where it is absorbed and refracted), and out onto the target chamber wall.

To understand what happens to the ray on its path from the beam to the chamber wall, it is necessary to understand what goes on within the target during an implosion. As the target implodes, a gradually increasing region of plasma forms outside the target called the corona. The electron density within the corona increases as the center of the target is approached. Eventually a density is reached that is so high that no light can penetrate beyond this point within the corona. This place is called the critical surface.

Rays enter the target from the beam at various angles of incidence with respect to the radial direction that determine how far into the corona each ray travels (Figure 1). As the ray enters the corona, its energy starts being absorbed. More of the laser light gets absorbed in areas with higher electron density. Rays that enter the target on the beam axis travel to the critical surface, and therefore travel further into the corona than any other rays. These rays are refracted straight back with most of their energy absorbed. Rays entering the target at angles that are close to the beam axis travel through the corona but never reach the critical surface and are refracted through the corona until they exit at an acute angle with the beam axis. Rays that enter the target further from the beam axis travel through the low-density part of the corona and are not absorbed much; they exit the target at an obtuse angle.

The reflected energy (not absorbed) of the rays from a single beam is distributed in concentric circles around the target chamber wall from the beam entrance to the opposite side. Rays that originate in the outer part of the beam emerge from the target at about 150°-160° to the incoming beam direction (0° corresponds to the rays that are reflected straight back) and yield the most reflected laser light because of their low absorption. Rays at about 165°-180° are produced only early in the pulse when the beam diameter is slightly larger than the initial target diameter and the corona has not yet expanded to a diameter larger than that of the beam. Although the rays that hit the target on axis are the most intense, they produce a very small amount of reflected laser light, because they are highly absorbed. When the corona is formed, none of the rays can pass to the other side of the target; this produces a shadow on the opposite side on the target chamber wall. This is illustrated in Fig. 1.

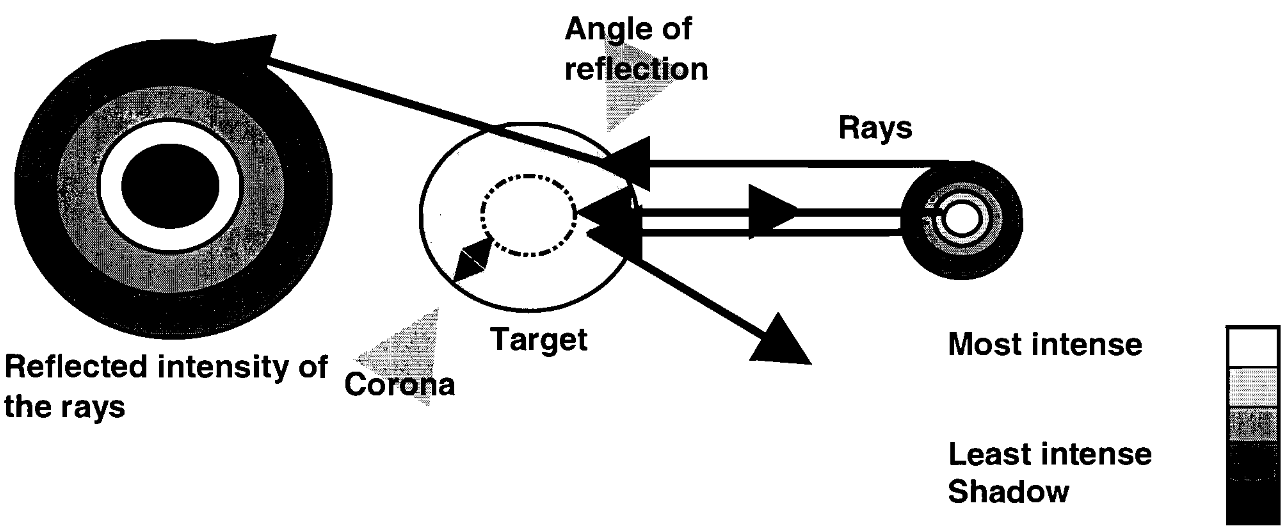

Figure 1: Ray trajectory and distribution of the light on the chamber wall for a single beam.

The intensity distribution from a single beam was calculated. Since all beams produce the same amount of light energy and are refracted similarly in the target, the intensity distribution from one beam can be used to map the distribution from all 60 beams on the chamber wall by transforming the reflected light distribution of a single beam to the position of all the beams on the wall. Intensity contributions from all beams were added to obtain a map of the total intensity distribution of the reflected laser light on the target chamber wall.

Program

A computer program was written in Fortran to calculate and map the intensity distribution of the reflected laser light.

The target chamber is set in the XYZ plane. The rays are generated in the UVW frame, which is the frame of a given beam. The radius of the chamber wall was arbitrarily set to 1 unit. Each kth ray from the UVW frame is reflected as a circle onto the chamber wall, with the angle of reflection β_K. The intensity of the reflected rays was calculated. For this simulation 200 rays for each beam were used. The boundary angle B_K of the concentric rays was calculated as the half way angle between the angles of rays β_K and β_{K+1}.

The circles that appear on the chamber wall from the reflected rays are divided into a θ-Φ grid on the target chamber wall with a resolution of one degree. Phi (Φ) represents the azimuthal angle within the XY plane and theta (θ) the declination angle within the ZX plane. This grid is used to map each ray into the XYZ frame. This is done by first finding the positions of each grid point of each ray in the UVW frame, transforming them into the XYZ plane using the direction cosines of the beam, and finally computing their angular position in the XYZ plane.

Spherical coordinates and rotation matrices are used to determine the position of each ray. First, direction cosines for the transformation using the position angles of the beams are determined from a table of the positions of the beams (θ', Φ') provided by the OMEGA operations group. Two rotations are required for the transformation: about the Z-axis (azimuthal) and about the Y-axis (declination):

$$\begin{pmatrix} \text{Direction} \\ \text{Cosines} \end{pmatrix} = \begin{pmatrix} \cos(\Phi') & \sin(\Phi') & 0 \\ -\sin(\Phi') & \cos(\Phi') & 0 \\ 0 & 0 & 1 \end{pmatrix} \bullet \begin{pmatrix} \cos(\theta') & 0 & \sin(\theta') \\ 0 & 1 & 0 \\ -\sin(\theta') & 0 & \cos(\theta') \end{pmatrix}$$

Rotation around: z-axis y-axis

The equations below use the calculated direction cosines to transform the ray positions from the UVW frame to the XYZ frame.

$$\begin{pmatrix} U \\ V \\ W \end{pmatrix} = \begin{pmatrix} \rho\sin(\theta)\cos(\Phi) \\ \rho\sin(\theta)\sin(\Phi) \\ \rho\cos(\theta) \end{pmatrix} \qquad \begin{pmatrix} X \\ Y \\ Z \end{pmatrix} = \begin{pmatrix} \text{Direction} \\ \text{Cosines} \end{pmatrix} \bullet \begin{pmatrix} U \\ V \\ W \end{pmatrix}$$

The following equations were used to calculate Phi and Theta in the XYZ frame:

$\theta_2 = \text{acos}(Z/\rho)$ $\Phi_2 = \text{atan}(Y/X)$,

where $\rho^2 = X^2 + Y^2 + Z^2$.

The program takes into account that more than one angle may have the same cosine and tangent values and includes an algorithm that ensures that the correct Phi and Theta values are calculated.

The intensity and the area on the chamber wall where the ray's intensity would be distributed were determined using the following equations:

$B_K = (\beta_K + \beta_{K+1})/2$

$A_K = 2\pi\rho^2(\cos(B_K) - \cos(B_{K-1}))$

$I_K = E_K/A_K$

where A_K is the area of the concentric ring formed by the reflected ray K, I_K, the intensity of the ray at the tank wall, ρ, the radius of the tank wall (set to unity), B_K, the angle of the boundary between rays and E_K, the energy of the reflected ray, obtained from LILAC.

The intensity distribution for each beam was calculated at a given time during the implosion. Fig. 2 shows intensity as a function of the angle of reflection of the rays within a single beam. The steep drop in intensity from 165° to 180° is due to the shadow of the target. At this time the diameter of the corona is larger than that of the beam. Rays that are reflected from the target at angles below 90° are the inner rays of the beam and have a low intensity because they travel the longest distances through the highest densities in the corona and are highly absorbed. Rays at about 150°-165° are the outer rays of the beam that travel through the low density of the corona and thus are not highly absorbed; also there is a higher density of reflected rays at those angles than at lower angles.

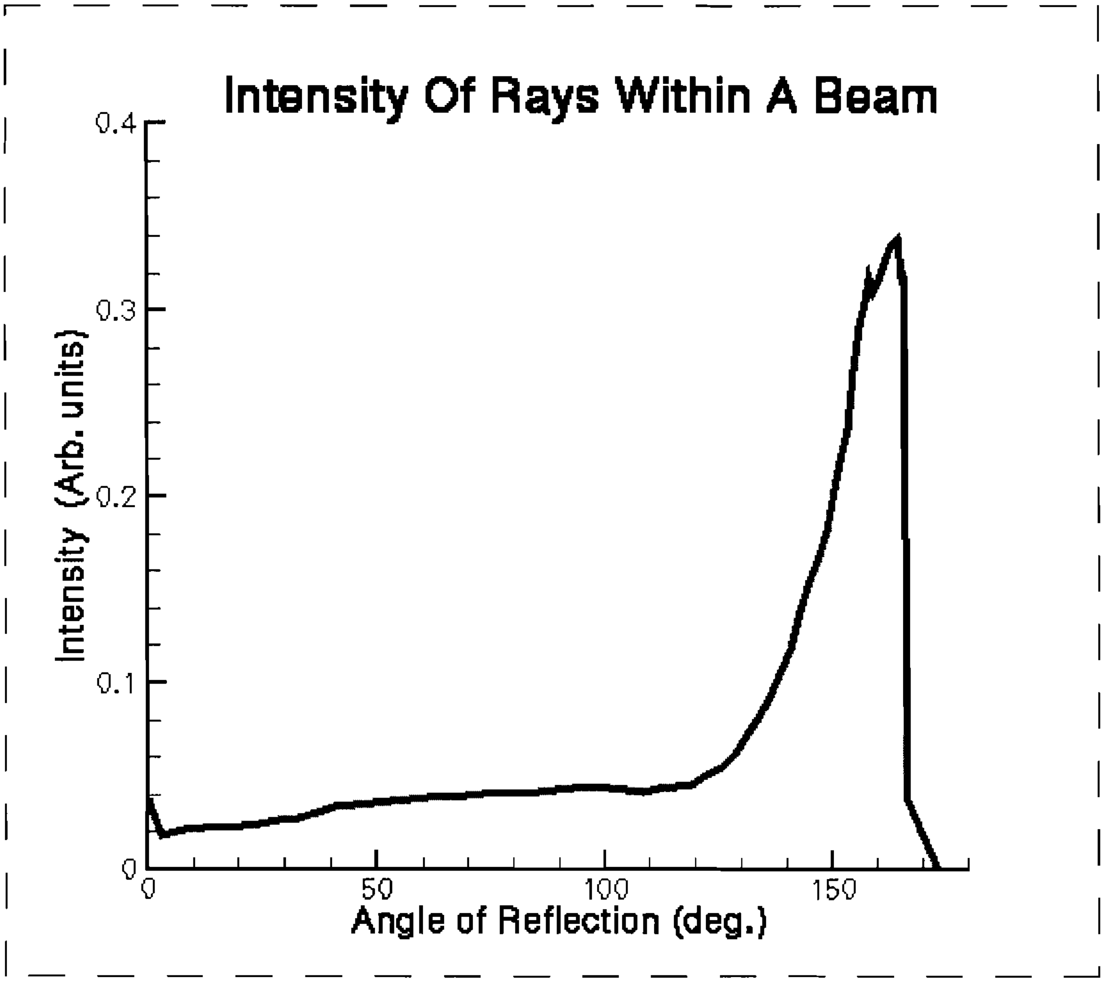

Figure 2: Intensity of the reflected rays from a single beam on the chamber wall.

The total intensity distribution of the reflected laser light along the target chamber wall is obtained by summing the intensity distributions of all 60 beams. Figure 3 is the map of the total intensity distribution of the reflected laser light integrated over the 1-ns pulse of the simulation.

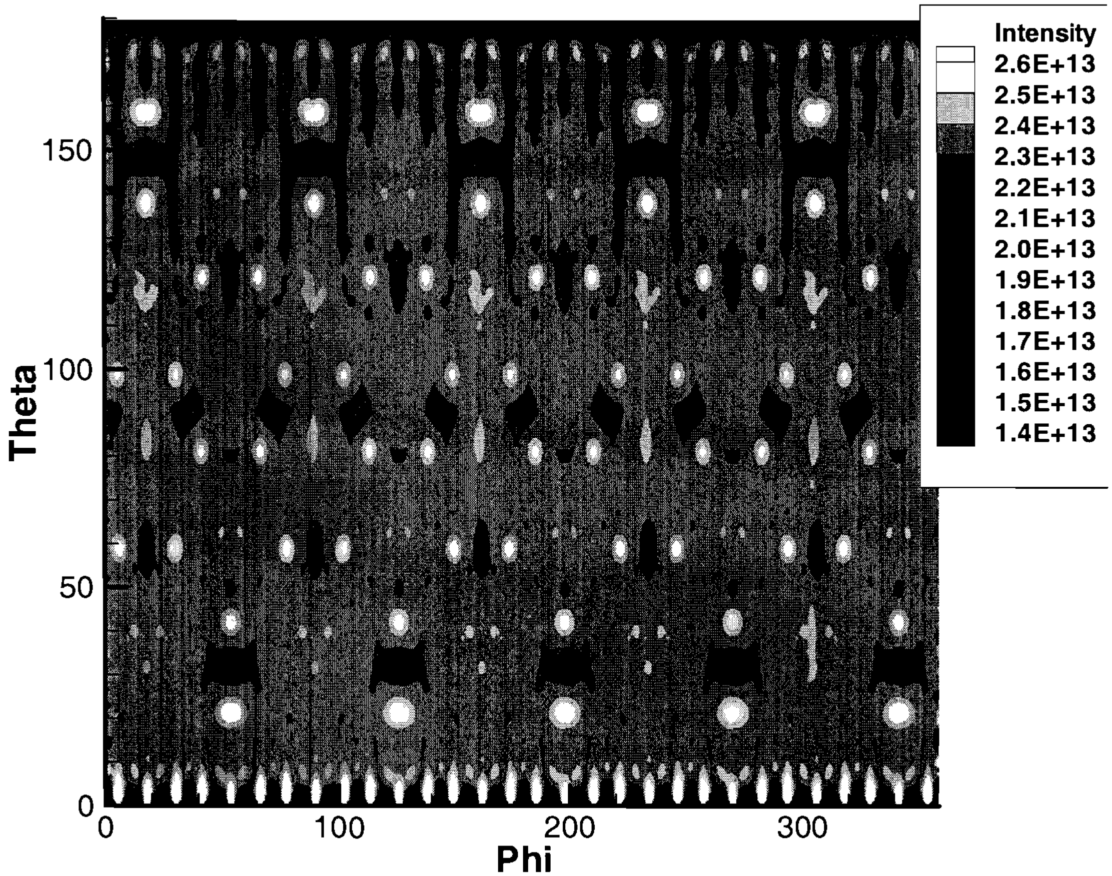

Figure 3: Mapping the 60 beams on the tank wall results in large-scale intensity non-uniformities of about ±5%.

The light areas on the graph represent regions of the tank wall with the highest intensity of the reflected laser light and the dark areas represent regions with the least intensity. The small bright regions result from the rays missing the target early, before the formation of a corona, and collected in the opposite beam lens. The noise at the top and the bottom of the map is due to the use of the simplest mapping methods to generate this graph. From the main part of the graph we can conclude that there is about ±5% peak-to-peak non-uniformity in the reflected light distribution.

Acknowledgements

My advisor, Dr. Jacques Delettrez, has put a lot of time and effort into helping me with this project. I greatly appreciate his patience, advice and guidance. I would also like to acknowledge Dr. Andrei Maximov, Joseph Dudek and Laurie Graham for advice on computer programming, rotational matrices, or help on the computer.